# A large-scale wetland cover change using time series Landsat imagery on Google Earth Engine: A case study in Newfoundland

M. Mahdianpari [a,b], H. Jafarzadeh [c], J. E. Granger [a], F. Mohammadimanesh [a], B. Brisco[d], B. Salehi [e], S. Homayouni[f] and Q. Weng [g]

[a]C-CORE, St. John's, Canada;
[b]Dept. of Electrical and Computer Eng., Memorial University of Newfoundland, St. John's, Canada;
[c]School of Surveying and Geospatial Engineering, College of Engineering, U. of Tehran, Tehran, Iran;
[d]The Canada Centre for Mapping and Earth Observation, Ottawa, Canada;
[e]Environmental Resources Engineering, College of Environmental Science and Forestry, State University of New York, USA;
[f]Institut National De La Recherche Scientifique, Centre Eau Terre Environnement, Quebec City, Canada;
[6]Center for Urban and Environmental Change, Department of Earth and Environmental Systems, Indiana State University, Terre Haute, IN, USA

**Abstract**

Wetlands across Canada have been, and continue to be, lost or altered under the influence of both anthropogenic and natural activities, such as land development and climate change. The ability to assess the rate of change to wetland ecosystems and related spatial pattern dynamics is important for effective and meaningful wetland management and protection. Given the impacts of climate change across the globe, now more than ever, it is of benefit to assess such patterns at large and encompassing scales, e.g., regional or national scales for an entire country. The availability of cloud-based geospatial platforms such as the Google Earth Engine has allowed for the production of countrywide wetland maps, yet change to these wetlands at the wetland class scale has yet to be implemented. This study assessed 30 years of change to wetlands across the province of Newfoundland using Landsat imagery to demonstrate this possibility. Assessment of change was successful at the wetland class scale, including bog, fen, swamp, and marsh, elucidating patterns in wetland change across Newfoundland from 1985 to 2015. The results of this study demonstrate the potential of GEE and Landsat historical imagery to not only assess change at both provincial and national levels of the entire country of Canada.

## 1. Introduction

Climate change is amongst the most significant challenges faced by northern countries in modern times. The current and predicted catastrophic impacts of a warming climate on various ecosystems had been reported extensively, including in Canada, where climate change has the potential to cause increasing instances of fire and impacts on the ability of ecosystems to recover from natural disasters [1], permafrost melt [2], and alterations to ecosystem extent and

vegetation structure [3], among others. Such impacts highlight the need for efficient and timely adaptation to climate change. A preliminary step for effective climate change adaptation is to monitor changes to precious ecosystems located within these countries to mitigate or at least reduce the adverse effects of current and future climate change.

Wetlands are amongst the most valuable and productive resources on the globe and provide numerous hydrological and ecological services, such as global climate regulation, natural water purification, flood and drought amelioration, shoreline erosion protection, soil conservation, opportunities for recreation and aesthetic appreciation, and wildlife habitat [4–7]. Although the definition of wetlands depends mainly on the scientific field of study, they can be simply defined as areas inundated or saturated by water for at least part of the year [8,9].

Wetlands and the services they provide are under the direct and indirect influence of anthropogenic activity [10–12], resulting in amplified rates of wetland change and loss [13]. Since the beginning of the 20th century, about two-thirds of the wetlands have been lost or severely altered [14]. Such loss has not only resulted in a decrease in global wetland coverage but has impacted the provision of valuable wetland services to humans and non-humans alike [15]. In Canada, historical causes of wetland loss included land-use change due to development and agriculture and associated bi-products such as re-direction of run-off and pollution[16]. In modern times, however, climate change can amplify ongoing wetland loss and change [17–19]. Due to wetlands' valuable and irreplaceable environmental services, constant monitoring and mapping changes to wetlands in current times play a crucial role in effective management, conservation, and restoration of these essential ecosystems [6,20]. In addition, change detection in wetland areas could be essential for assessing past and future trends, developing evidence-based policy and preventing future disaster events [21].

Due to the wetlands ecosystem's dynamic nature, conducting conventional vegetation, water, and soil sampling for monitoring wetlands is difficult and time-consuming, requiring extensive fieldwork and sustainable human involvement over large geographic areas [9,20,22]. In contrast, remote sensing is an efficient tool that can play a key and constructive role in assessing and studying wetland status and measuring the extent of wetland changes on both long-term and large-scales [23,24]. Utilizing optical satellites is an effective and valid alternative in vegetation monitoring and assessing the change of wetland areas [25]. The archived moderate resolution Landsat time-series data provides an exclusive opportunity to detect and identify wetland changes resulting from the extensive historic imagery library [22].

Due to a lack of sufficient satellite data and computing resources, most studies applying change detection techniques do so over only small areas [26]. With the recent availability of the Google Earth Engine (GEE), an integrated cloud-computing platform for remote sensing and Earth science data processing [26,27], it is now possible to investigate and apply change detection algorithms at large regional scales for land cover change research (such as exploring wetland

dynamics) at multi-spatial and -temporal resolutions [27,28]. The GEE solves computer intensive problems and provides a quickly accessible collection of ready-to-use data products, including long-term Landsat imagery series, Sentinel datasets, etc., as well as advanced machine learning tools to handle and manipulate big earth observation data for large areas [29,30].

Remote sensing has increasingly been used to produce ecosystem maps, land-cover change information, and track ecosystem status over large-scales and long-period observation [31]. In the literature, there exist several studies dealing with land cover change detection at small and large-scales using bi-temporal and multi-temporal data. The proposed methods are mainly categorized as algebra-based, transformation-based, and classification-based methods [32–34]. Image classification-based approaches widely used in land use/land cover change detection, provide detailed change information within the study area [34]. This category contains two main subcategories, including direct multi-date classification methods, wherein just one classifier is used for stacking multi-temporal data sets, and post-classification methods in which two or more data sets are separately classified and then compared [35,36].

Several studies have developed change detection strategies on the GEE platform. In [26] a new approach was proposed to generate and update land change maps via a combination of the CART, CVAPS methods and NDVI time series analysis for the western regions of China. Sidhu and her colleagues in [30] evaluated and demonstrated the usefulness of GEE as a web-based remote sensing platform for detecting land cover changes for Urban areas in Singapore [30]. The Breaks For Additive Season and Trend (BFAST) method has been used to investigate cropping systems and temporal paddy crop dynamics in Sidoarjo Regency, Indonesia, and provides accurate and up-to-date information on agricultural land-use changes [37]. In [38], the result of large-scale and long-term change patterns over a cropland area near Dongting Lake in China was characterized via the LandTrendr algorithm with Landsat time-series data derived from GEE [38].

Many other studies have applied change detection strategies to the specific case studies of wetland ecosystems. For example, [39] examined monthly coastal dynamics in the Zhoushan Archipelago using GEE, a full time-series of Landsat imagery, and the Modified Normalized Difference Water Index, noting a loss of coastal tidal flats and establishing the potential of GEE for use in monitoring other coastal wetland areas. [40] used a Landsat time series to determine change and type conversion of wetland areas in the Willamette River floodplain in Oregon, finding that wetland loss slowed after the implementation of wetland-related policy in the area, demonstrating the importance of change detection techniques for examining the effectiveness of wetland policies and management decisions. Similarly, [41] quantified an increase in coastal emergent marsh wetland because of wetland restoration efforts, again demonstrating the importance of change detection providing evidence for the usefulness of wetland mitigation strategies. Of particular relevance, [42] successfully assed changes to treed and non-treed wetlands across 650 million hectares of Canada's forested ecosystems between 1984 and 2016.

To build on these methods, ours will be the first study to apply a change detection technique within the GEE to monitor changes of wetlands across the province of Newfoundland at the level of wetland class (bog, fen, swamp, and marsh). The methods discussed here will support further assessment of change to wetland class at the scale of the entire country of Canada. The main objectives of this study are to (1) explore the feasibility of detecting wetland class and land cover changes using Landsat imagery and associated vegetation features, (2) monitoring and understanding wetland cover dynamics over time, and (3) determining causes of change to the wetlands.

## 2. Materials and methods

### 2.1. Study area

The study area encompasses the entire island of Newfoundland, located on the eastern-most coast of Canada (Figure 1). Within its 108,860 $km^2$ area is a highly diverse landscape, characterized by a range of climate, geology and vegetation. As such, various land cover typifies the Newfoundland landscape, including dense boreal forest, rolling heath, and sprawling peatlands. The current anthropogenic land cover makes up roughly 11% of the island's total area, with the largest concentration in and amongst the capital city of St. John's and a number of other cities and communities, including Corner Brook, Gander, Grand Falls-Windsor, and Deer Lake.

Wetlands are a dominant feature of the Newfoundland landscape, making up an estimated 18% of the total land cover, the majority of which are peatlands, including bog and fen [43]. While there has been extensive work dedicated to establishing the current extent of wetlands across the island [44,45], there exists very little information as it regards to past and future trends of wetland loss and change. Rough estimates state that around 80-98% of wetlands in and around Canadian cities and two-thirds of coastal marsh in Atlantic Canada have been lost since the time of settlement [46,47]. However, the specifics of wetland loss and change in Newfoundland are not yet known. Likely causes for historical wetland loss and change on the island include wetland drainage and conversion to urban or agricultural land-use. Similar pressures are likely to drive future trends in wetland loss and change, though climate change is a confounding factor [18,19].


**Figure 1.** The Island of Newfoundland and the locations of field-collected reference data.

Field data were collected across Newfoundland during the summers of 2015-2017 and provided the basis for the multi-year reference datasets used later in the change detection methodology. During 2015-2017, numerous wetlands were visited by biologists and ecologists in and around several communities across Newfoundland, including St. John's (east coast), Deer Lake (central), Grand Falls-Windsor (central), and Gros Morne (west coast). The distribution and locations of the reference data collected from 2015 to 2017 are presented in Figure. These areas were selected as they best represent landscapes common across Newfoundland while also containing various roadways accessing as many wetlands as efficiently possible over a short amount of time. While in the field, wetlands were classified as bog, fen, swamp, or marsh based on the as guidelines by the Canadian Wetland Classification System (National Wetlands Working Group, 1997). Ultimately 432 wetlands with a size greater than or equal to one hectare were classified and later digitized into polygons, creating a wetland training dataset for the years 2015-2017. Additional land cover classes, such as urban, pasture, forest, and water were, including, resulting in a reference dataset containing 817 polygons. Figure 2 shows a more detailed view of the distribution of training data.

The 2015-2017 dataset was used as the basis for the creation of an additional three datasets representing wetland and non-wetland land cover across the island during the years of 1985-

1987, 1995-1997, and 2005-2007. To do this, each of the 817 polygons from the 2015-2017 were compared with historical reports, maps, aerial photo, and Landsat imagery of the relevant dates (1985-1987, 1995-1997, and 2005-2007). Polygon classes and polygon boundaries were modified or removed, where any past land cover changes had occurred. For example, several marsh polygon boundaries were modified as water levels and vegetation growth through the years changed. Similarly, various urban polygons present in the 2015-2017 datasets were removed as the urban landscapes in the past tended to be less extensive. If dramatic differences in the appearance of wetland vegetation across the years was noticed, as was sometimes the case where a fen had dried and became more swamp-like, the polygon was removed or reclassified if possible. In cases where a polygon was removed, another polygon representing land cover of the same type was delineated elsewhere to ensure that the multi-year datasets had similar total polygon and area counts.

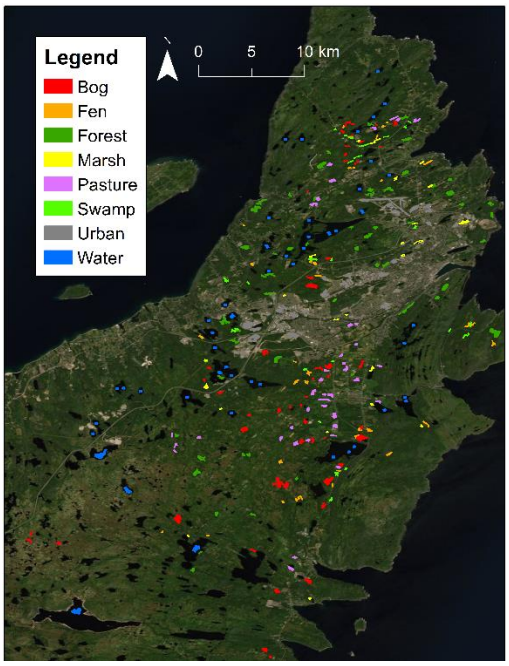


St. John's

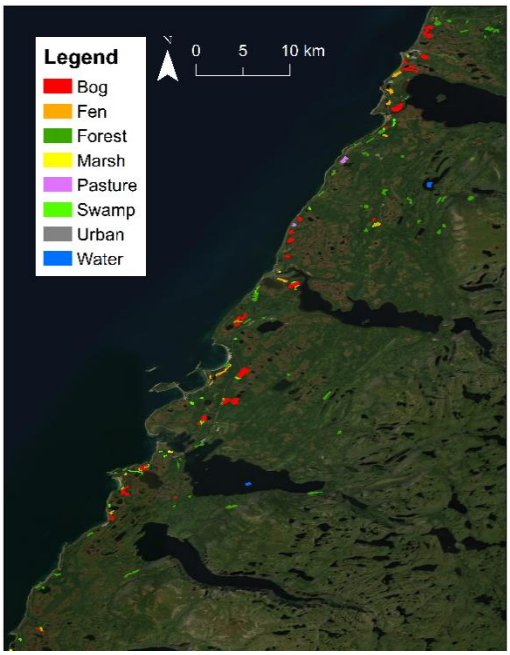


Gros Morne

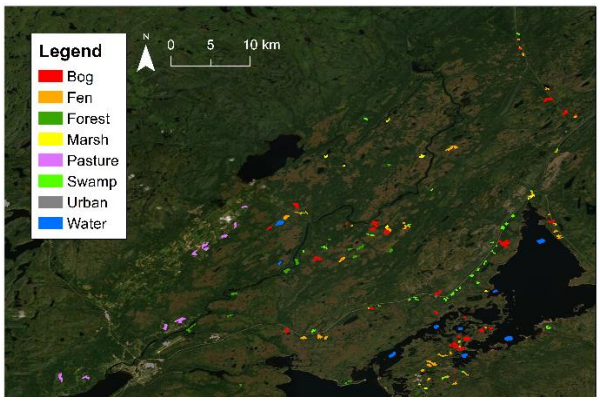


Deer Lake

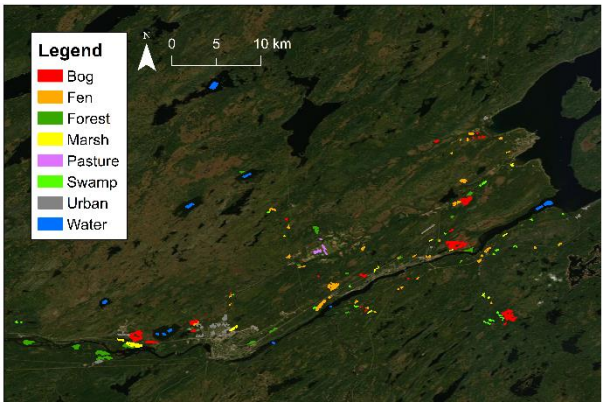


Grand Falls-Windsor

**Figure 2.** Reference wetland and non-wetland data collected in and around the St. John's, Gros Morne, Deer Lake, and Grand Falls-Windsor areas of Newfoundland.

171

172 2.2. Data collection and pre-processing

173

174 In our study, surface reflectance Tier 1 data product of three different types of Landsat images
175 (Landsat 5, 7 and 8) from 1985-2017 were obtained from the USGS earth explorer website on
176 GEE platform. Table 1 summarizes the specifications of the data used in this study. Although the
177 Landsat archive contains remotely sensed imagery, which was continuously acquired since 1972,
178 frequent cloud cover results in excessive temporal gaps in the Landsat data, for certain regions,
179 especially in wetland areas or during specific time periods. In order to achieve the study
180 objectives and prepare cloud-free composites, each composite was created using the minimal
181 cloud cover and overlapped images of three consecutive years [1985-1987, 1995-1997, 2005-
182 2007, 2015-2017] taken from June 1 to October 30. Finally, four composites from 284 images,
183 including 135 TM (Thematic Mapper), 50 ETM+ (Enhanced Thematic Mapper Plus), and 99 OLI
184 (Operational Land Imager) with almost free cloud cover were prepared to contain the median
185 reflectance values of the collections. Moreover, since 2003, due to failure of the scan-line
186 corrector (SLC) of ETM+ imager on Landsat 7, approximately 22% of the pixels of ETM+ images
187 have no data [28]. A common method to fill no data stripes is utilizing SLC-off gaps filling method
188 [48], but in this case, some of the stripes may not get filled due to the cloud cover threshold
189 employed in each composite. To deal with this problem, the third image composite was created
190 by the means of both Landsat 5 and Landsat 7 images. Note that the similar bands of different
191 Landsat sensor types (TM, ETM+ and OLI/TIRS), including Blue, Green, Red, NIR, SWIR1, SWIR2
192 and TIR bands, were chosen and stacked to create composites. Additionally, to improve the
193 classification results, the spectral indices, including DVI, NDVI, GDVI, GNDVI, GRVI, GSAVI,
194 GOSAVI, SAVI, OSAVI, EVI, NDWI, TasselledCap_Wet, TasselledCap_Veg were calculated and
195 added to the composites. In addition, these composites contain one band consisting of the
196 Shuttle Radar Topography Mission (SRTM) V4 digital elevation for providing elevation data of the
197 study site. The selected bands and indices were used as input features for the classification.
198 Figure 3 illustrates the number of Landsat observations over the summer of the aforementioned
199 years.

200

201 **Table 1.** The number of Landsat imagery and cloud cover threshold employed in each composite.

202

| Composite | Period | Landsat satellite | Number of Images | Cloud cover |
|---|---|---|---|---|
| First | 1985-1987 | Landsat 5 TM | 62 | <20 % |
| Second | 1995-1997 | Landsat 5 TM | 46 | <10 % |
| Third | 2005-2007 | Landsat 7 ETM+ | 50 + | <15 % |

| | | | | |
|---|---|---|---|---|
| | | Landsat 5 TM | 27 | |
| Fourth | 2015-2017 | Landsat 8 OLI/TIRS | 99 | <20% |

203

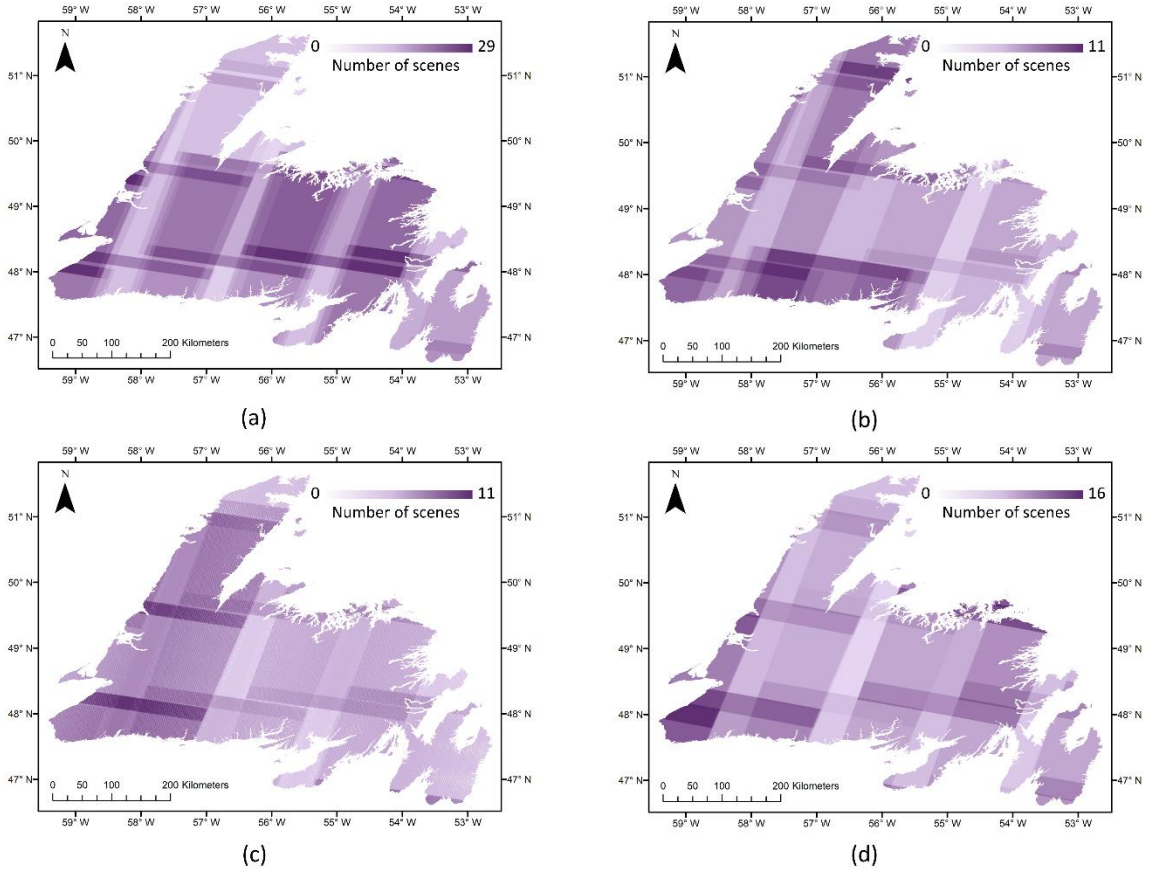


204

205 **Figure 3.** Distribution and number of Landsat scenes in (a) the first, (b) second, (c) third, and (d)
206 fourth image composites used in this study.

207

208 2.3. Post-classification change detection

209 This study intents to develop a land cover map that satisfies the requirements for a wetland
210 change detection application. We performed the detection of wetland change regions in the GEE.
211 In this study, the pixel-based classification of multi-temporal composites was produced to assess
212 change regions and prepare change maps. The available classification algorithms within GEE
213 include Classification and Regression Tree (CART), decision tree (DT), random forest (RF), support
214 vector machine (SVM), etc. We executed pixel-based classification with RF tree-based classifier
215 that works by growing a number of random decision trees to full depth. The RF model is a well-
216 known ensemble classifier that effectively distinguishes between spectrally similar land covers.

The robustness of this algorithm has been proven in the literature [49]. The important user-specified variables in RF include the number of Rifle decision trees to create per class, the number of variables per split and the minimum size of a terminal node [50]. Once the classification model was applied to the composites of sequential times, pixel-by-pixel comparing of classified maps generated change maps.

### 2.4. Validation and Accuracy assessment

To provide error analysis and assessment of classified maps, and consequently, the change detection results, overall accuracy (OA) rate, which is the portion of cases that were classified correctly, user's accuracy (UA) and producer's accuracy (PA) were estimated based on confusion matrices. The user's accuracy is defined as the accuracy of the classification despite commission errors, which occur when pixels in obtained classes are ascribed to a particular class that, in fact, does not belong to it. Furthermore, the producer's accuracy is defined as the accuracy of classification despite errors of omission, which occurs when pixels belonging to one class are included in other classes [51,52].

## 3. Results

Figure 4 shows the distribution of land cover classes across Newfoundland for each time-period, and figure 5 shows the total coverage of each land cover class as calculated from the final classifications. Based on these results, bog and forest are consistently the most dominant wetland and non-wetland land in Newfoundland for all years, respectively. These results are consistent with other reports of dominant Newfoundland land cover [44,53]**.** Marsh is consistently the least common wetland class, having the lowest coverage of any wetland class during all periods. Other reports of Newfoundland wetlands that note the rareness of marsh reflect the findings presented here [53]**.** Agriculture and urban/barren are the least common land cover classes overall. These results are as expected as the majority of the Newfoundland landscape has not been altered by human modifications.

Bog wetland coverage is the lowest during the earliest years studied (the 80s and the 90s), and highest in the most recent (2000s). The fen and swamp results reflect this trend somewhat, with fen having the lowest coverage in the 80s and swamp in the 90s. The total amount of the marsh class, however, seems to alternate between years, being highest in the 80s and early 2000s and lowest in the 90s and late 2000s. Bog coverage is far more extensive than all other wetland classes during every time period. Swamp is the second most extensive wetland class for all periods except the 90s, during which fen is more extensive. Based on Figure 4, peatlands, including bog and fen, are most common in the middle and southern portions of the island, while forest dominants along the west and north coasts.

The result of the accuracy assessment of the classified maps is shown in Table 2. The 2015-2017 classification had the highest overall accuracy at 88%, followed by the 2005-2007 classification

at 85%, the 1985-1987 classification at 84% and the 1995-1997 classification at 83%. Generally, across all time periods, non-wetland land-use had the highest user and producer accuracies between 91 to 100%. Of the wetland classes, bog had the overall highest producer's accuracies between 92% to 97%, and fen had the highest user's accuracies between 66% to 86%. Marsh generally had higher user and producers accuracy values compared to that of the swamp, which had the lowest accuracy results of all classes, wetland and non-wetland.

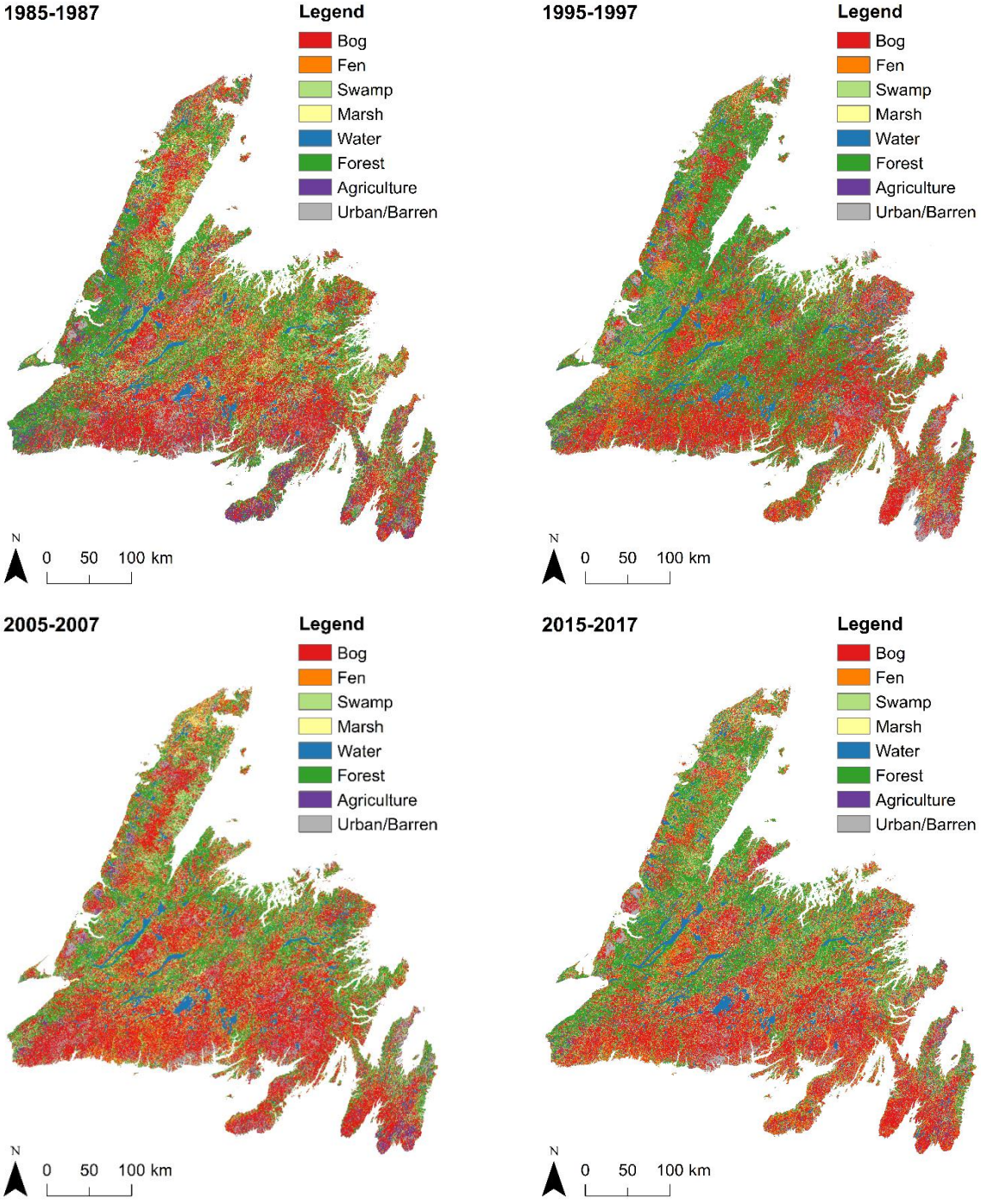

**Figure 4.** Wetland and non-wetland land cover classification using Landsat imagery from 1985-1987 (top left), 1995-1997 (top right), 2005-2007 (bottom left) and 2015-2017 (bottom right).

**Table 2.** Accuracy assessment of classified maps based on the error matrix.

| *Composite* | *Estimator* | *Bog* | *Fen* | *Swamp* | *Marsh* | *Water* | *Forest* | *Pasture* | *Urban* |
|---|---|---|---|---|---|---|---|---|---|
| *First* | ***PA*** | 94.28 | 44.45 | 35.0 | 50.0 | 95.34 | 92.06 | 88.89 | **94.54** |
| | ***UA*** | 80.48 | 85.71 | 58.33 | 42.85 | 100 | 84.05 | 100 | **97.14** |
| | ***OA*** | **84.72** | | | | | | | |
| *Second* | ***PA*** | 92.40 | 51.61 | 8.33 | 42.85 | 96.29 | 91.83 | 100 | **94.87** |
| | ***UA*** | 78.49 | 66.66 | 20.0 | 75.0 | 100 | 86.53 | 86.66 | **97.36** |
| | ***OA*** | **83.26** | | | | | | | |
| *Third* | ***PA*** | 96.97 | 36.84 | 62.50 | 62.50 | 97.72 | 91.42 | 100 | **93.54** |
| | ***UA*** | 73.56 | 82.35 | 50.0 | 62.15 | 100 | 91.63 | 94.11 | **100** |
| | ***OA*** | **85.40** | | | | | | | |
| *Fourth* | ***PA*** | 94.11 | 53.33 | 47.05 | 50.0 | 100 | 98.27 | 100 | **100** |
| | ***UA*** | 82.05 | 80.0 | 57.14 | 62.50 | 100 | 89.06 | 100 | **100** |
| | ***OA*** | **88.21** | | | | | | | |

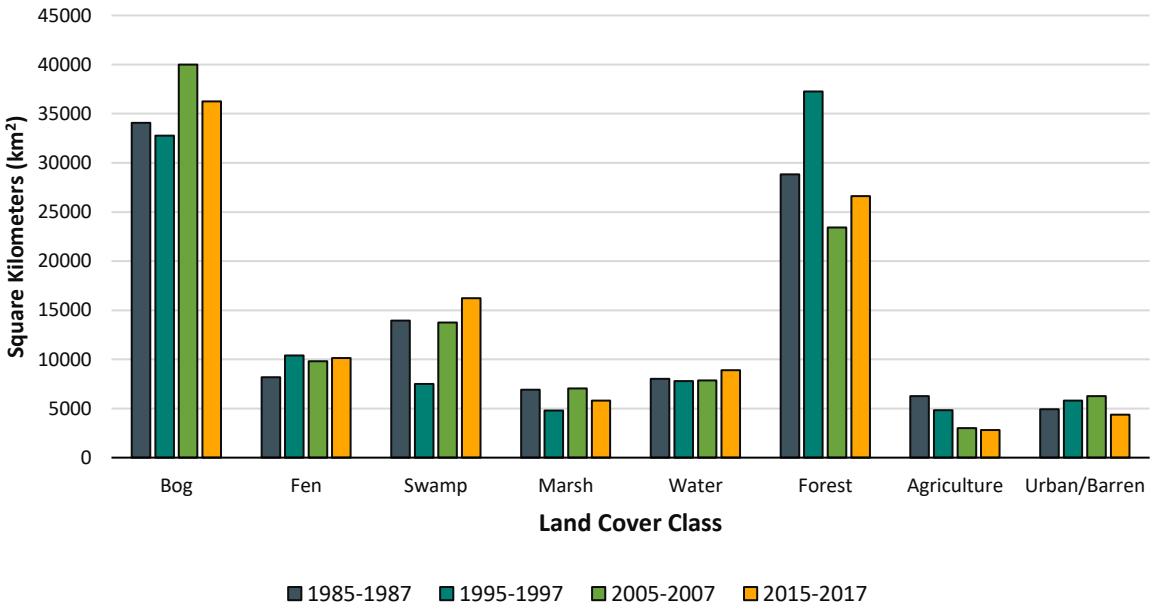


**Figure 5.** The total area of each wetland and non-wetland land cover class per period of time.

Random Forests are not only used for prediction but also to assess and determine the importance of each variable in the classification scheme. The variable importance analysis is a bi-product of RF classification and determines the contribution of each predictor variable to the general classification model. Figure 6 illustrated the normalized importance variable of extracted features

in this study. As shown, the TIR band and SRTM elevation data were the essential features for wetland classification in different years, followed by NDWI and DVI indices. It is interesting to see that the same features play approximately the same role in the classification of different composites.

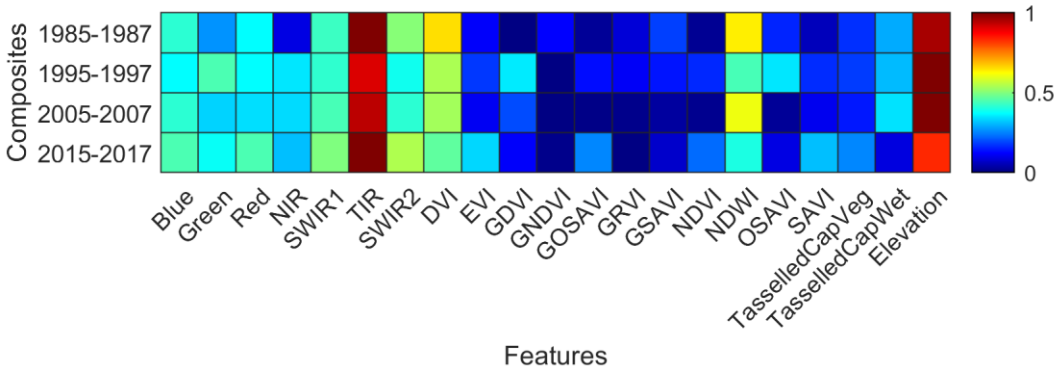


**Figure 6.** Heat map of the variable importance for the four classified maps of

Figures 7, 8, and 9 show the total amount of wetland coverage lost and gained between the 80s and the 90s, between the 90s and the early 2000s, and between the early 2000s and the late 2000s, respectively. Overall, the time-period between the 80s and 90s was the only time during which there was a net loss of wetlands as a single class. The results also show a net gain of wetlands as a single class between the 90s and the early 2000s, and between the early 2000s and late 2000s.

Between the 80s and 90s (Figure 7), all wetland classes except for fen experienced a net loss in coverage, with swamp experiencing the most significant decrease. Much of the swamp loss during this time period appears to be a result of conversion into forest areas. Similarly, the loss of bog is mostly a result of conversion to fen. Between the 90s and the early aughts (figure 8), fen coverage experienced a small net loss while bog, swamp and marsh experienced a net gain, respectively. The gain in swamp brought its total area back to a similar level, as was present in the 80s (Figure 7). Between the early and late aughts (Figure 9), bog and marsh experienced a net loss, while swamp experienced a net gain. Fen also experienced a small net gain.

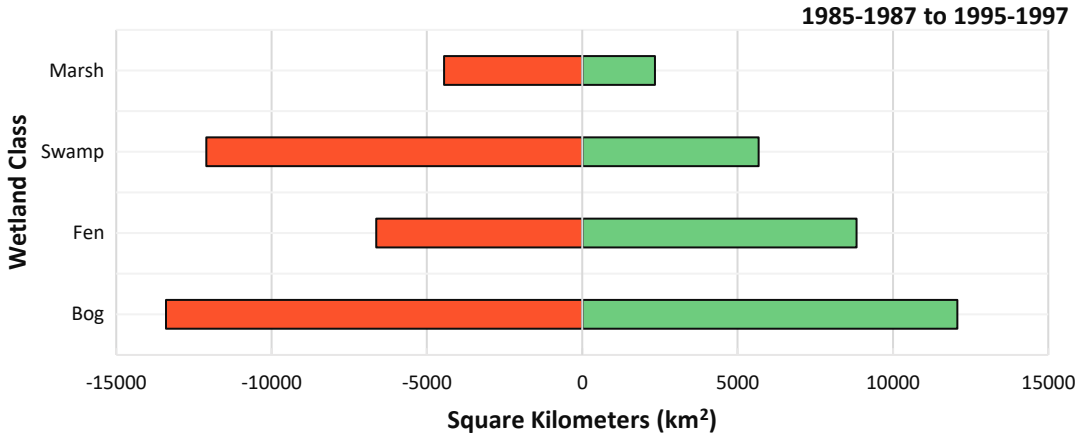


**Figure 7.** Loss and gain of wetland class land coverage between the 1980s and the 1990s.

283

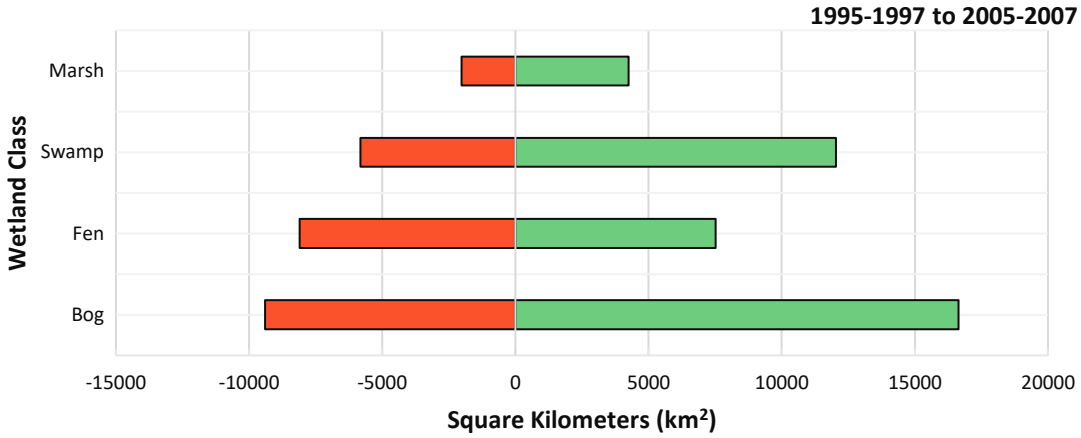


**Figure 8.** Loss and gain of wetland class land coverage between the 1990s and the early 2000s.

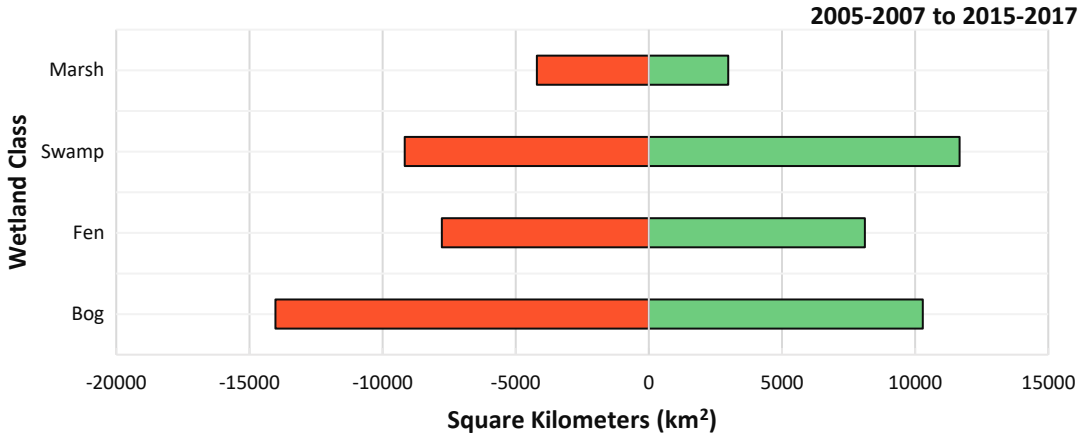


**Figure 9.** Loss and gain of wetland class land coverage between the early and late 2000s.

284

285 Figure 10 shows the total amount of wetland coverage lost due to conversion to anthropogenic
286 land cover, including agriculture and urban (Figure 10a), other wetland classes (figure 10b), and

non-wetland natural land cover, including forest and water (Figure 10c). Generally, the most significant contributor to the loss within an individual wetland class seems to be the conversion to another wetland class, particularly in the case of bog and fen. Bog, for example, is often lost because of conversion to the fen class and vice versa, though a substantial amount of bog and fen has also converted to upland forest. Based on the results in Figure 10b, the loss within a wetland class because of a conversion to another class is most prominent between the early and late 2000s. While a large portion of swamp and marsh loss seems to be a result of wetland class conversion, an even more substantial portion is driven by conversion to non-anthropogenic upland classes such as forest and open water (Figure 10c). A greater amount of total marsh and swamp area is lost to the conversion to non-anthropogenic upland than bog or fen.

Conversion of wetlands to non-anthropogenic upland is most prominent between the 80s and 90s, and least prominent between the 90s and the 2000s. Compared to other categories of land cover (wetland and non-anthropogenic upland), the conversion of wetlands to anthropogenic classes is less common (figure 10a). The most considerable loss of wetlands to anthropogenic land cover seems to have occurred between the 80s and the 90s. The lowest amount of bog and fen conversion to anthropogenic land cover occurred most recently, between the early and late 20000s. Conversely, loss of swamp and marsh to anthropogenic land cover seems to have increased slightly during this time period.

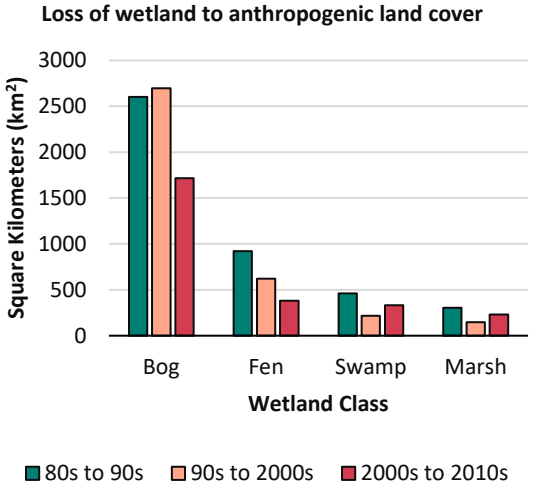


(a)

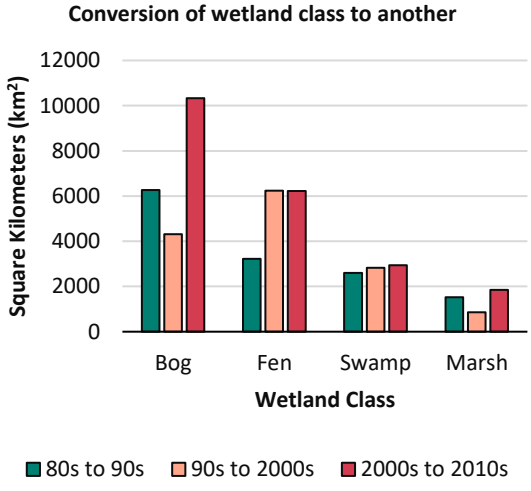


(b)

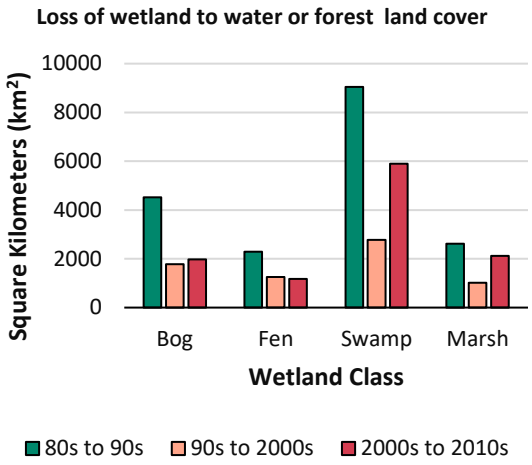


**(c)**

**Figure 10.** (a) Conversion of wetlands to anthropogenic land cover including urban and agriculture, (b) conversion of one wetland class to another, and (c) conversion of wetlands into the forest or water land cover.

Table 3 and Figure 11 provide information about the amount and location of wetlands that remained stable or unstable across time periods. Stable wetland areas are those wetland classes that remained the same class across time. Unstable wetlands areas are those areas that were classified as a wetland, became a wetland, or changed wetland class. Generally, a majority of areas experienced wetland instability compared to wetland stability (Table 2). This is also the case for individual wetland classes. For example, for all time periods, the area of stable swamp is less than areas of unstable swamp presence. All time periods experienced greater instability and less stability, at similar rates. Specifically, there is 38, 936 $km^2$ more unstable wetland area than the stable area between the 80s and 90s, 35, 662 $km^2$ more unstable wetland area than the stable area between the 90s and the early 2000s, and 32, 829 $km^2$ more unstable wetland area versus stable area between the early and late 2000s. Note, however, that instability seems to decrease slightly in the recent years.

**Table 3.** Area of wetland class that has changed and area of wetland class that remained unchanged between time periods.

| | 1985-1987 to 1995-1997 | | 1995-1997 to 2005-2007 | | 2005-2007 to 2015-2017 | |
|---|---|---|---|---|---|---|
| *Wetland Class* | ***Unchanged ($km^2$)*** | ***Changed ($km^2$)*** | ***Unchanged ($km^2$)*** | ***Changed ($km^2$)*** | ***Unchanged ($km^2$)*** | ***Changed ($km^2$)*** |
| Bog | 20683 | 25465 | 23350 | 26039 | 25966 | 24309 |
| Fen | 1558 | 15463 | 2284 | 15623 | 2022 | 15898 |
| Swamp | 1838 | 17774 | 1697 | 17858 | 4568 | 20839 |
| Marsh | 2471 | 6784 | 2791 | 6264 | 2840 | 7179 |

| | | | | | | |
|---|---|---|---|---|---|---|
| Total Wetland | 26550 | 65486 | 30122 | 65784 | 35396 | 68225 |

321


**Figure 11.** Areas where a wetland class remained unchanged over time (green), and areas that were or became a wetland (purple).

322

323 **4. Discussion**

Though there has been extensive work recently dedicated to the mapping and classification of Newfoundland's wetlands [44, 45, 54] there has been little information regarding rates of wetland loss and gain over time. This information is pertinent for informing on the effectiveness of government policies and for assessing the potential impacts of climate change and changing local populations and industry. Additionally, assessing changes to coverage of wetland classes allows for an indirect assessment of the loss and gain of valuable wetland services, many of which are tied directly to wetland class [55]. The results of this work help elucidate various trends in wetland change over 30 years on the island of Newfoundland, explicitly reporting on gains and loss of specific wetland classes, including bog, fen, swamp and marsh. While working on the wetland change detection have already been conducted across Canada [42], none thus far have been conducted in Newfoundland, nor at the scale of the wetland class.

Based on the results of this work, several patterns of interest have arisen. For example, the major cause for wetland class loss across Newfoundland is the conversion from one wetland class to another, or conversion to a non-anthropogenic upland class (see figures 10 b and c). While the conversion of a wetland class to another is sometimes a natural part of a wetlands succession, as is exemplified by the conversion of fen to bog [56], accelerated or substantial rates of class conversion may also be a result of climate change, or a result of anthropogenic modifications to the landscape [18,57]. Peatlands such as bog and fen, for example, may experience drying as a result of increased temperatures, decreased precipitation, and modified water flow and water tables [17,58]. This drying will, in turn, allow for the establishment of woody vegetation over time, resulting in the conversion of bog or fen to the swamp.

Similarly, the injection of excess nutrients into a bog, via pollution in the air or run-off, may result in a shift in vegetation from bog-like to fen-like [59,60]. Notably, much of the loss of bog and fen wetland coverage in Newfoundland is attributed to the conversion to swamp or upland forest, or the conversion of bog and fen alternatively. Similarly, the results show that the loss of marsh and swamp wetlands is primarily due to conversion to open water and forest, respectively. This also may be due in part to climate change, where-by a warming climate, for example, may cause some swamps to dry, becoming more similar in vegetation composition to the upland forest.

While climate change is likely a contributing factor to such changes in wetlands across Newfoundland, additional confounding factors should be considered when interpreting these results. For one, separating swamp from the upland forest has always been a difficult challenge, mainly when using lower resolutions [61]. Thus, there is potential for some misclassification between swamp and forest amongst several years examined in this research, causing there is a misrepresentative amount of swamp loss to forest and vice versa. This problem is commonly solved by adding Synthetic Aperture Radar (SAR) data to the classification methodology. SAR imagery with longer wavelengths, such as ALOS imagery, is recommended. This is because SAR signals with longer wavelengths can penetrate through vegetation canopy, capturing the

structure below and thus providing more information for allowing for the discrimination between the swamp and upland forest.

Similarly, much marsh vegetation is emergent, and its growth is closely related to local weather patterns and the growing season, which may vary from year to year. Additionally, if a satellite image captures a marsh on a particularly wet day, after too much rain, for example, a marsh may appear to be flooded entirely with little to no exposed vegetation, resulting in a classification of open water and a recorded loss of marsh wetlands. Confusion between bog and fen classes is also a common problem in wetland classification, as many bog and fen share very similar vegetation patterns [43,62,63]. Such information on the dynamics of wetlands and the difficulties associated with their classification must be considered when interpreting change detection of wetland classes, and when drawing any conclusion as to the cause of wetland loss over time.

The results of this work establish a justification for the assessment of wetland change detection at the level of class across the entirety of Canada's landscape using the GEE and Landsat imagery over the past 30 years. While there has been work dedicated to assessing wetland change patterns across Canada previously [42] and work towards assessing the current extents of wetland classes across the country [4], there has yet to be an attempt to assess countrywide change at the level of the wetland class. Information on rates of change to wetland classes may not only help to elucidate impacts of climate change across the country but also allow for a more in-depth assessment of the loss and modification of class-specific wetland services. Such information will also allow for the fair assessment and comparison of various federal and provincial based wetland protection and management policies across Canada.

## 5. Conclusion

Understanding large-scale wetland dynamics is of great importance in the era of global climate change and information exchange. Knowledge of change to wetlands, at the class level, is of particular importance due to the class-related services that these wetlands provide, such as improving the lives of humans and non-human animals alike. At the time of realizing this research, there has not yet been an analysis to detect large-scale wetland change at the class level in Canada. As such, the objective of this research was to support the potential of such application by investigating the feasibility and applicability of historical Landsat imagery and GEE cloud-computing platform on a large scale and time basis, over a single province in Canada. In particular, we used available machine learning algorithms in the GEE platform and Landsat surface reflectance data to detect wetland classes and understand wetland land cover dynamics over time.

The results of this study provide for the first time, an assessment of wetland spatial dynamics across the entirety of Newfoundland at the level of the wetland class. The results reveal that bog, fen, swamp, marsh, water, forest, pasture and urban have experienced significant instability

over the past 30 years, mostly because of climate change and anthropogenic activities. These results support the further application of these methods to a future change detection study of the entirety of Canada and confirm the usefulness of the archived Landsat images in the GEE for monitoring long-term wetland dynamics over the past three decades. Such information will allow stakeholders to not only compare statistics as it relates to wetland gain and loss but also allow for the comparison of the effectiveness and quality of province-based wetland policies, which in turn may allow for the general improvement of these policies across the country.

As wetlands are susceptible to multiple factors, including climate change, population growth, and land-use conversion, it is necessary to develop effective policies for the process of wetland protection and restoration. Based on the potential of the Landsat data archive and GEE cloud-computing platform, in a future study, we plan to use this approach for the entire country of Canada in hopes of contributing to the expansion of knowledge of as it relates to Canadian wetlands and wetland conservation.

## References


1. Boucher, D.; Gauthier, S.; Thiffault, N.; Marchand, W.; Girardin, M.; Urli, M. How climate change might affect tree regeneration following fire at northern latitudes: a review. *New For.* **2020**, *51*, 543–571, doi:10.1007/s11056-019-09745-6.
2. MacDonald, S.; Birchall, S.J. Climate change resilience in the Canadian Arctic: The need for collaboration in the face of a changing landscape. *Can. Geogr. Géographe Can.* **2019**, cag.12591, doi:10.1111/cag.12591.
3. Sulphur, KC; Goldsmith, S.A.; Galloway, J.M.; Macumber, A.; Griffith, F.; Swindles, GT; Patterson, R.T.; Falck, H.; Clark, I.D. Holocene fire regimes and treeline migration rates in sub-arctic Canada. *Glob. Planet. Change* **2016**, *145*, 42–56, doi:10.1016/j.gloplacha.2016.08.003.
4. Mahdianpari, M.; Mohammadimanesh, F.; Brisco, B.; Homayouni, S.; Gill, E.; R. DeLancey, E.; Bourgeau-Chavez, L. Big Data for a Big Country: The First Generation of Canadian Wetland Inventory Map at a Spatial Resolution of 10-m Using Sentinel-1 and Sentinel-2 Data on the Google Earth Engine Cloud Computing Platform. *Canadian Journal of Remote Sensing* **2020**, *46*.
5. Tiner, R.W.; Lang, M.W.; Klemas, V.V. *Remote sensing of wetlands: applications and advances*; CRC press, 2015;
6. Xu, T.; Weng, B.; Yan, D.; Wang, K.; Li, X.; Bi, W.; Li, M.; Cheng, X.; Liu, Y. Wetlands of International Importance: Status, Threats, and Future Protection. *Int. J. Environ. Res. Public. Health* **2019**, *16*, 1818.
7. Fang, C.; Tao, Z.; Gao, D.; Wu, H. Wetland mapping and wetland temporal dynamic analysis in the Nanjishan wetland using Gaofen One data. *Ann. GIS* **2016**, *22*, 259–271, doi:10.1080/19475683.2016.1231719.

8. Tiner, R.W. *Wetland Indicators: A Guide to Wetland Formation, Identification, Delineation, Classification, and Mapping, Second Edition*; CRC Press, 2016; ISBN 978-1-4398-5370-2.
9. Kaplan, G.; Avdan, U. Monthly analysis of wetlands dynamics using remote sensing data. *ISPRS Int. J. Geo-Inf.* **2018**, *7*, 411.
10. Mitsch, W.J.; Gosselink, J.G. The value of wetlands: importance of scale and landscape setting. *Ecol. Econ.* **2000**, *35*, 25–33, doi:10.1016/S0921-8009(00)00165-8.
11. Mitsch, W.J.; Gosselink, J.G. *Wetlands, 4th editio*; John Wiley & Sons, Inc., Hoboken, New Jersey, 2007;
12. Gibbes, C.; Southworth, J.; Keys, E. Wetland conservation: change and fragmentation in Trinidad's protected areas. *Geoforum* **2009**, *40*, 91–104.
13. Syphard, AD; Garcia, M.W. Human-and beaver-induced wetland changes in the Chickahominy River watershed from 1953 to 1994. *Wetlands* **2001**, *21*, 342–353.
14. Connor, R. *The United Nations world water development report 2015: water for a sustainable world*; UNESCO publishing, 2015; Vol. 1;.
15. Gardner, R.C.; Barchiesi, S.; Beltrame, C.; Finlayson, C.; Galewski, T.; Harrison, I.; Paganini, M.; Perennou, C.; Pritchard, D.; Rosenqvist, A. State of the world's wetlands and their services to people: a compilation of recent analyses. **2015**.
16. Byun, E.; Finkelstein, S.A.; Cowling, S.A.; Badiou, P. Potential carbon loss associated with post-settlement wetland conversion in southern Ontario, Canada. *Carbon Balance Manag.* **2018**, *13*, 6, doi:10.1186/s13021-018-0094-4.
17. Breeuwer, A.; Robroek, B.J.M.; Limpens, J.; Heijmans, M.M.P.D.; Schouten, M.G.C.; Berendse, F. Decreased summer water table depth affects peatland vegetation. *Basic Appl. Ecol.* **2009**, *10*, 330–339, doi:10.1016/j.baae.2008.05.005.
18. von Sengbusch, P. Enhanced sensitivity of a mountain bog to climate change as a delayed effect of road construction. *Mires Peat* **2015**, *15*, 1–18.
19. Edvardsson, J.; Šimanauskienė, R.; Taminskas, J.; Baužienė, I.; Stoffel, M. Increased tree establishment in Lithuanian peat bogs — Insights from field and remotely sensed approaches. *Sci. Total Environ.* **2015**, *505*, 113–120, doi:10.1016/j.scitotenv.2014.09.078.
20. Ayanlade, A.; Proske, U. Assessing wetland degradation and loss of ecosystem services in the Niger Delta, Nigeria. *Mar. Freshw. Res.* **2016**, *67*, 828–836.
21. Thonfeld, F.; Feilhauer, H.; Braun, M.; Menz, G. Robust Change Vector Analysis (RCVA) for multi-sensor very high resolution optical satellite data. *Int. J. Appl. Earth Obs. Geoinformation* **2016**, *50*, 131–140.
22. Huang, H.; Chen, Y.; Clinton, N.; Wang, J.; Wang, X.; Liu, C.; Gong, P.; Yang, J.; Bai, Y.; Zheng, Y. Mapping major land cover dynamics in Beijing using all Landsat images in Google Earth Engine. *Remote Sens. Environ.* **2017**, *202*, 166–176.
23. Mabwoga, S.O.; Thukral, A.K. Characterization of change in the Harike wetland, a Ramsar site in India, using landsat satellite data. *SpringerPlus* **2014**, *3*, 576.

24. McCarthy, M.J.; Merton, E.J.; Muller-Karger, F.E. Improved coastal wetland mapping using very-high 2-meter spatial resolution imagery. *Int. J. Appl. Earth Obs. Geoinformation* **2015**, *40*, 11–18.
25. Identifying wetland change in China's Sanjiang Plain using remote sensing | SpringerLink Available online: https://link.springer.com/article/10.1672/08-04.1 (accessed on Apr 15, 2020).
26. Hu, Y.; Dong, Y. An automatic approach for land-change detection and land updates based on integrated NDVI timing analysis and the CVAPS method with GEE support. *ISPRS J. Photogramm. Remote Sens.* **2018**, *146*, 347–359.
27. Liu, D.; Chen, N.; Zhang, X.; Wang, C.; Du, W. Annual large-scale urban land mapping based on Landsat time series in Google Earth Engine and OpenStreetMap data: A case study in the middle Yangtze River basin. *ISPRS J. Photogramm. Remote Sens.* **2020**, *159*, 337–351.
28. Wu, L.; Li, Z.; Liu, X.; Zhu, L.; Tang, Y.; Zhang, B.; Xu, B.; Liu, M.; Meng, Y.; Liu, B. Multi-Type Forest Change Detection Using BFAST and Monthly Landsat Time Series for Monitoring Spatiotemporal Dynamics of Forests in Subtropical Wetland. *Remote Sens.* **2020**, *12*, 341.
29. Mutanga, O.; Kumar, L. Google Earth Engine Applications. *Remote Sens.* **2019**, *11*, 591, doi:10.3390/rs11050591.
30. Sidhu, N.; Pebesma, E.; Câmara, G. Using Google Earth Engine to detect land cover change: Singapore as a use case. *Eur. J. Remote Sens.* **2018**, *51*, 486–500, doi:10.1080/22797254.2018.1451782.
31. author, DLC; Mausel, P.; Brondízio, E.; Moran, E. Change detection techniques. *Int. J. Remote Sens.* **2004**, *25*, 2365–2401, doi:10.1080/0143116031000139863.
32. Bovolo, F.; Bruzzone, L. A theoretical framework for unsupervised change detection based on change vector analysis in the polar domain. *IEEE Trans. Geosci. Remote Sens.* **2006**, *45*, 218–236.
33. Nielsen, A.A. The regularized iteratively reweighted MAD method for change detection in multi-and hyperspectral data. *IEEE Trans. Image Process.* **2007**, *16*, 463–478.
34. Hussain, M.; Chen, D.; Cheng, A.; Wei, H.; Stanley, D. Change detection from remotely sensed images: From pixel-based to object-based approaches. *ISPRS J. Photogramm. Remote Sens.* **2013**, *80*, 91–106.
35. Singh, A. Review article digital change detection techniques using remotely-sensed data. *Int. J. Remote Sens.* **1989**, *10*, 989–1003.
36. Nemmour, H.; Chibani, Y. Multiple support vector machines for land cover change detection: An application for mapping urban extensions. *ISPRS J. Photogramm. Remote Sens.* **2006**, *61*, 125–133.
37. Fatikhunnada, A.; Seminar, KB; Liyantono, L.; Solahudin, M.; Buono, A. Optimization of Parallel K-means for Java Paddy Mapping Using Time-series Satelite Imagery. *TELKOMNIKA*

*Telecommun. Comput. Electron. Control* **2018**, *16*, 1409–1415, doi:10.12928/telkomnika.v16i3.6876.
38. Zhu, L.; Liu, X.; Wu, L.; Tang, Y.; Meng, Y. Long-Term Monitoring of Cropland Change near Dongting Lake, China, Using the LandTrendr Algorithm with Landsat Imagery. *Remote Sens.* **2019**, *11*, 1234, doi:10.3390/rs11101234.
39. Cao, W.; Zhou, Y.; Li, R.; Li, X. Mapping changes in coastlines and tidal flats in developing islands using the full time series of Landsat images. *Remote Sens. Environ.* **2020**, *239*, 111665, doi:10.1016/j.rse.2020.111665.
40. Fickas, KC; Cohen, W.B.; Yang, Z. Landsat-based monitoring of annual wetland change in the Willamette Valley of Oregon, USA from 1972 to 2012. *Wetl. Ecol. Manag.* **2016**, *24*, 73–92, doi:10.1007/s11273-015-9452-0.
41. Ballanti, L.; Byrd, K.; Woo, I.; Ellings, C. Remote Sensing for Wetland Mapping and Historical Change Detection at the Nisqually River Delta. *Sustainability* **2017**, *9*, 1919, doi:10.3390/su9111919.
42. Wulder, M.A.; Li, Z.; Campbell, E.M.; White, J.C.; Hobart, G.; Hermosilla, T.; Coops, NC. A National Assessment ofWetland Status and Trends for Canada's Forested Ecosystems Using 33 Years of Earth Observation Satellite Data. *Remote Sens.* **2018**, *10*, 1623.
43. National Wetlands Working Group *The Canadian wetland classification system*; Wetlands Research Branch, University of Waterloo: Waterloo, Ont., 1997; ISBN 978-0-662-25857-5.
44. Mahdianpari, M.; Salehi, B.; Mohammadimanesh, F.; Homayouni, S.; Gill, E. The First Wetland Inventory Map of Newfoundland at a Spatial Resolution of 10 m Using Sentinel-1 and Sentinel-2 Data on the Google Earth Engine Cloud Computing Platform. *Remote Sens.* **2018**, *11*, 43, doi:10.3390/rs11010043.
45. Mohammadimanesh, F.; Salehi, B.; Mahdianpari, M.; Motagh, M. A New Hierarchical Object-Based Classification Algorithm for Wetland Mapping in Newfoundland, Canada. In Proceedings of the IGARSS 2018 - 2018 IEEE International Geoscience and Remote Sensing Symposium; IEEE: Valencia, 2018; pp. 9233–9236.
46. Austen, E.; Hanson, A. An Analysis of Wetland Policy in Atlantic Canada. *Can. Water Resour. J.* **2007**, *32*, 163–178, doi:10.4296/cwrj3203163.
47. *Water Policy and Governance in Canada*; Renzetti, S., Dupont, D.P., Eds.; Global Issues in Water Policy; Springer International Publishing: Cham, 2017; Vol. 17; ISBN 978-3-319-42805-5.
48. Chen, J.; Zhu, X.; Vogelmann, J.E.; Gao, F.; Jin, S. A simple and effective method for filling gaps in Landsat ETM+ SLC-off images. *Remote Sens. Environ.* **2011**, *115*, 1053–1064.
49. de Sousa, C.; Fatoyinbo, L.; Neigh, C.; Boucka, F.; Angoue, V.; Larsen, T. Cloud-computing and machine learning in support of country-level land cover and ecosystem extent mapping in Liberia and Gabon. *PloS One* **2020**, *15*, e0227438.

50. Goldblatt, R.; You, W.; Hanson, G.; Khandelwal, AK Detecting the boundaries of urban areas in india: A dataset for pixel-based image classification in google earth engine. *Remote Sens.* **2016**, *8*, 634.
51. Kelley, L.C.; Pitcher, L.; Bacon, C. Using Google Earth engine to map complex shade-grown coffee landscapes in Northern Nicaragua. *Remote Sens.* **2018**, *10*, 952.
52. Jafarzadeh, H.; Hasanlou, M. An Unsupervised Binary and Multiple Change Detection Approach for Hyperspectral Imagery Based on Spectral Unmixing. *IEEE J. Sel. Top. Appl. Earth Obs. Remote Sens.* **2019**, *12*, 4888–4906.
53. Buchanan, R.A.; Houlihan, T. St. John's Waterways and Wetlands: An environmental policy study. 1987.
54. Mahdianpari, M.; Salehi, B.; Mohammadimanesh, F.; Motagh, M. Random forest wetland classification using ALOS-2 L-band, RADARSAT-2 C-band, and TerraSAR-X imagery. *ISPRS J. Photogramm. Remote Sens.* **2017**, *130*, 13–31, doi:10.1016/j.isprsjprs.2017.05.010.
55. Hanson, A.R.; Canadian Wildlife Service; Atlantic Region *Wetland ecological functions assessment: an overview of approaches*; Canadian Wildlife Service: Ottawa, 2008; ISBN 978-1-100-11499-6.
56. Tiner, R.W. *Wetland Indicators (Second Edition). A Guide to Wetland Formation, Identification, Delineation, Classification, and Mapping.*; CRC Press: Boca Raton, Florida, 2017;
57. Pasquet, S.; Pellerin, S.; Poulin, M. Three decades of vegetation changes in peatlands isolated in an agricultural landscape. *Appl. Veg. Sci.* **2015**, *18*, 220–229, doi:10.1111/avsc.12142.
58. Potvin, L.R.; Kane, E.S.; Chimner, R.A.; Kolka, R.K.; Lilleskov, E.A. Effects of water table position and plant functional group on plant community, aboveground production, and peat properties in a peatland mesocosm experiment (PEATcosm). *Plant Soil* **2015**, *387*, 277–294, doi:10.1007/s11104-014-2301-8.
59. Hedwall, P.-O.; Brunet, J.; Rydin, H. Peatland plant communities under global change: negative feedback loops counteract shifts in species composition. *Ecology* **2017**, *98*, 150–161, doi:10.1002/ecy.1627.
60. Nishimura, A.; Tsuyuzaki, S. Plant responses to nitrogen fertilization differ between post-mined and original peatlands. *Folia Geobot.* **2015**, *50*, 107–121, doi:10.1007/s12224-015-9203-2.
61. Jahncke, R.; Leblon, B.; Bush, P.; LaRocque, A. Mapping wetlands in Nova Scotia with multi-beam RADARSAT-2 Polarimetric SAR, optical satellite imagery, and Lidar data. *Int. J. Appl. Earth Obs. Geoinformation* **2018**, *68*, 139–156, doi:10.1016/j.jag.2018.01.012.
62. Bourgeau-Chavez, L.L.; Endres, S.; Powell, R.; Battaglia, M.J.; Benscoter, B.; Turetsky, M.; Kasischke, E.S.; Banda, E. Mapping boreal peatland ecosystem types from multitemporal

radar and optical satellite imagery. *Can. J. For. Res.* **2017**, *47*, 545–559, doi:10.1139/cjfr-2016-0192.

63. Touzi, R.; Deschamps, A.; Rother, G. Wetland characterization using polarimetric RADARSAT-2 capability. *Can. J. Remote Sens.* **2007**, *33*, 12.